Optical Organophosphate Sensor Based upon Gold Nanoparticle Functionalized Fumed Silica Gel

ARTICLE *in* ANALYTICAL CHEMISTRY · JUNE 2007

Impact Factor: 5.64 · DOI: 10.1021/ac062165h · Source: PubMed

3 AUTHORS, INCLUDING:

Janelle Newman
MRIGlobal-Midwest Research Institute
6 PUBLICATIONS **248** CITATIONS
SEE PROFILE

Gary J Blanchard
Michigan State University
187 PUBLICATIONS **3,969** CITATIONS
SEE PROFILE

Optical Organophosphate Sensor Based upon Gold Nanoparticle Functionalized Fumed Silica Gel

J. D. S. Newman, J. M. Roberts, and G. J. Blanchard*

Department of Chemistry, Michigan State University, East Lansing, Michigan 48824

We report on the creation of a high surface area, chemically selective material for the efficient adsorption of organophosphate and organophosphonate species. Using silica microparticles in conjunction with gold nanoparticles and surface modification chemistry, we have demonstrated a material with a binding constant for organophosphonates and organophosphates (OPPs) of $K = 2 \times 10^6$ M^{-1}. The binding of OPPs to the modified gold nanoparticles appears as a spectral shift in the gold nanoparticle resonance. The sensitivity of this technique is limited by scattering losses of suspensions of the particles, and we report on how this sensitivity can be recovered to a significant extent by the use of solvents with a refractive index close to that of the silica particles.

Over the past several years, organophosphates and phosphonates (OPPs) have become increasingly important as analytes for several reasons. Many nerve agents and pesticides are organophosphates or organophosphonates, making the ability to detect small quantities or low concentrations of these compounds critically important. In certain cases, sequestration is desirable owing to the toxicity of the analyte. The ratification of the Chemical Warfare Convention (CWC) has underscored the need to develop rapid, sensitive, and selective detectors for chemical warfare agents and other organophosphate/phosphonate compounds in order to verify compliance with the provisions of the treaty.[1] Contamination of groundwater and agricultural products entering the human food chain by organophosphate/phosphonate pesticides has also led to the need for sensitive detection and sequestration methods.[2−9] We report here on the development of a high-surface area material based upon silica microparticles. The use of covalently attached gold nanoparticles (AuNPs) as a surface area enhancing scaffold and a foundation for surface modification chemistry allows for the creation of a high-affinity material that is selective primarily for OPP compounds.[10−13] Once the analytes have been sorbed onto this novel material, the coated silica particles can be suspended in a solvent and the AuNP plasmon resonance can be monitored with relatively high signal-to-noise ratio, depending on the choice of solvent. While there are technical challenges associated with this approach, we have chosen to use fumed silica in conjunction with AuNPs because the fumed silica can be suspended in aqueous and other solutions without aggregation for extended periods of time, unlike AuNPs, because silica microparticles are more amenable to physical separation methodologies, such as filtering, than AuNPs, and because this structural motif provides a relatively high surface-to-volume ratio to enhance the adsorption and sequestration of OPP species.

Current methods for detection of OPP compounds include chromatographic techniques,[14−19] mass spectrometric methods,[15,17] electrochemical detection,[3,6,7,20,21] biosensors,[3,7−9,20,21] and fluorescent beads.[22] While these techniques have many advantages, including sensitivity and selectivity, they are often time-consuming and labor-intensive. The ideal OPP sensor would possess the sensitivity and selectivity of the already-established methods and would reduce the dependence on expensive instrumentation. Robustness, simplicity, the ability to sequester the analyte of interest, and possible incorporation into existing air filtration schemes would be beneficial, and there are several recent examples of OPP sensors based on nanoparticles that begin to satisfy these requirements.[3,6,8,22] Both AuNPs and zirconium oxide nanoparticles have shown promise in the detection of OPPs.

* To whom correspondence should be addressed. E-mail: blanchard@chemistry.msu.edu.

(1) Organisation for the Prohibition of Chemical Weapons, 2005.
(2) Halamek, J.; Pribyl, J.; Makower, A.; Skladal, P.; Scheller, F. W. *Anal. Bioanal. Chem.* **2005**, *382*, 1904−1911.
(3) Hu, S.-Q.; Xie, J.-W.; Xu, Q.-H.; Rong, K.-T.; Shen, G.-L.; Yu, R.-Q. *Talanta* **2003**, *61*, 769−777.
(4) Janotta, M.; Karlowatz, M.; Vogt, F.; Mizaikoff, B. *Anal. Chim. Acta* **2003**, *496*, 339−348.
(5) Kunz, R. R.; Leibowitz, F. L.; Downs, D. K. *Anal. Chim. Acta* **2005**, *531*, 267−277.
(6) Liu, G.; Lin, Y. *Anal. Chem.* **2005**, *77*, 5894−5901.
(7) Liu, G.; Lin, Y. *Anal. Chem.* **2006**, *78*, 835−843.
(8) Simonian, A. L.; Good, T. A.; Wang, S. S.; Wild, J. R. *Anal. Chim. Acta* **2005**, *534*, 69−77.
(9) Wang, C.; Li, C.; Ji, X.; Orbulescu, J.; Xu, J.; Leblanc, R. M. *Langmuir* **2006**, *22*, 2200−2204.
(10) Chen, M. M. Y.; Katz, A. *Langmuir* **2002**, *18*, 8566−8572.
(11) Doron, A.; Katz, E.; Willner, I. *Langmuir* **1995**, *11*, 1313−1317.
(12) Shipway, A. N.; Katz, E.; Willner, I. *ChemPhysChem* **2000**, *1*, 18−52.
(13) Putvinski, T. M.; Schilling, M. L.; Katz, H. E.; Chidsey, C. E. D.; Mujsce, A. M.; Emerson, A. B. *Langmuir* **1990**, *6*, 1567−1571.
(14) Black, R. M.; Muir, B. *J. Chromatogr., A* **2003**, *1000*, 253−281.
(15) Hooijschuur, E. W. J.; Kientz, C. E.; Brinkman, U. A. T. *J. Chromatogr., A* **2002**, *982*, 177−200.
(16) Isetun, S.; Nilsson, U.; Colmsjoe, A.; Johansson, R. *Anal. Bioanal. Chem.* **2004**, *378*, 1847−1853.
(17) Kientz, C. E. *J. Chromatogr., A* **1998**, *814*, 1−23.
(18) Marx, S.; Zaltsman, A.; Turyan, I.; Mandler, D. *Anal. Chem.* **2004**, *76*, 120−126.
(19) Sega, G. A.; Tomkins, B. A.; Griest, W. H. *J. Chromatogr., A* **1997**, *790*, 143−152.
(20) Joshi, K. A.; Tang, J.; Haddon, R.; Wang, J.; Chen, W.; Mulchandani, A. *Electroanalysis* **2005**, *17*, 54−58.
(21) Wang, J.; Chen, G.; Muck, A.; Chatrathi, M. P.; Mulchandani, A.; Chen, W. *Anal. Chim. Acta* **2004**, *505*, 183−187.
(22) Bencic-Nagale, S.; Sternfeld, T.; Walt, D. R. *J. Am. Chem. Soc.* **2006**, *128*, 5041−5048.

Pavlov et al. have demonstrated the utility of AuNP plasmon resonance measurements for the optical determination of OPPs[23] and Liu and Lin[6] have demonstrated an OPP sensor based on the affinity of the analyte for ZrO_2 nanoparticles. In that work, the binding of the OPPs to the nanoparticles was determined electrochemically. In this work, we combine the chemical advantages of Liu's sensor with the simple detection scheme of Pavlov's sensor to create a high-surface-area optical sensor and sequestration medium for OPPs. The sensor/dosimeter methodology we report here utilizes several well-established chemical reactions to achieve relatively low level detection and OPP sequestration simultaneously.

The material and measurement methodology is based on a series of well-established silica and gold surface modification reactions. First, the silica gel is functionalized with a mercaptosilane,[24−27] followed by attachment of AuNPs by stirring the functionalized silica gel in an aqueous citrate-stabilized AuNP colloidal solution.[11,28−30] Following the attachment of AuNPs, the citrate stabilizer is displaced by exposing the silica-bound AuNPs to an ethanolic solution of an ω-hydroxythiol.[31] The hydroxyl termini on the AuNPs are then reacted with $POCl_3$, H_2O, and Zr^{4+} to form a zirconium−phosphate (ZP)-terminated surface. This chemistry was pioneered by the Mallouk, Thompson, and Katz groups,[13,25,32,33] and our group has made extensive use of ZP chemistry to grow robust interfacial films efficiently.[34−37] Because the ZP chemistry operates by using Zr^{4+} to link phosphate or phosphonate groups, the terminal Zr^{4+} ions on our modified AuNPs have a high affinity for OPPs.[6,35] We note that the ZP chemistry could be used directly on the silica gel to produce a surface with high affinity for OPPs, and it is possible that the chemistry we apply to the AuNPs could also react with any residual surface silanol groups on the silica gel. We have used AuNPs as optical reporting agents, where the plasmon resonance band of the AuNP is sensitive to the condition of the ZP linkage bound to its surface.

Both the material and the associated plasmon resonance detection methodology we report are useful in several regards. First, the covalent nature of the attachment chemistry makes it robust and able to be stored under ambient conditions. Second, the incorporation of AuNPs provides access to the plasmon resonance, a band that is remarkably sensitive to changes in the local dielectric environment of the AuNPs. We observe that the plasmon resonance band blue-shifts when OPPs bind to the ZP-modified particles and interpret these data in the context of two spectrally overlapped bands, rendering an apparent blue-shift. The magnitude of the observed spectral shift is independent of OPP concentration after its initial appearance at a threshold OPP concentration in the microgram/liter range, and we understand this behavior through a simple complexation model.

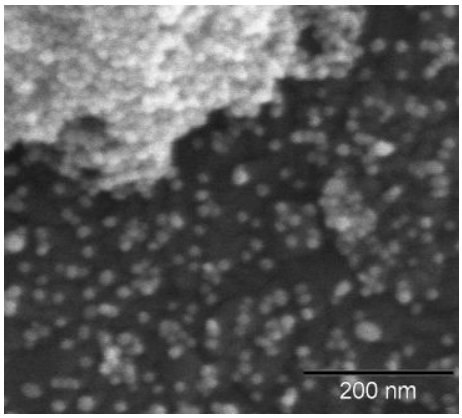

Figure 1. SEM image of AuNPs prepared by the citrate reduction method. Average particle size is 20 nm.

EXPERIMENTAL SECTION

Materials. Silica gel (Grade 633, 200−425 mesh, average surface area 480 m^2/g, with an average particle diameter of 63.6 μm, as determined by scanning electron microscopy, SEM) was purchased from Spectrum and used as received. Sodium citrate, hydrogen tetrachloroaurate ($HAuCl_4 \cdot 3H_2O$, 99.9+%), methylphosphonic acid (MPA), diethylchlorophosphate (DECP), and 3-mercaptopropyltrimethoxysilane (MPTMS) were purchased from Sigma-Aldrich and used as received. 6-Mercapto-1-hexanol and phosphorus oxychloride ($POCl_3$) were purchased from Fluka and used as received. Collidine was purchased from Spectrum and used as received. Zirconium(IV) oxychloride octahydrate ($ZrOCl_2 \cdot 8H_2O$) was purchased from Allied and used as received.

Preparation of AuNP Colloid. AuNPs were synthesized by reduction and stabilization with sodium citrate according to a modification of a published procedure.[38] A 1% (w/w) solution of $HAuCl_4 \cdot 3H_2O$ was added to a vigorously stirred aqueous solution of sodium citrate. The solutions were combined for an overall molar ratio of 3:1 sodium citrate/$HAuCl_4 \cdot 3H_2O$. The plasmon resonance band of the resulting colloid was centered at ~530 nm. SEM images of particles made using this method indicate an average particle size of 20 nm (Figure 1).

Silica Gel Functionalization. Silica gel (0.5 g) was placed into a round-bottom flask with an oval stir bar. A 5% (v/v) solution of MPTMS in toluene (10 mL) was added to the round-bottom flask and the resultant mixture stirred at room temperature for 24 h. The silica gel was filtered, rinsed with copious amounts of toluene and ethanol, and returned to a dry round-bottom flask. The aqueous solution of AuNPs (50 mL) was added to this round-

(23) Pavlov, V.; Xiao, Y.; Willner, I. *Nano Lett.* **2005**, *5*, 649−653.
(24) Goss, C. A.; Charych, D. H.; Majda, M. *Anal. Chem.* **1991**, *63*, 85−88.
(25) Kallury, K. M. R.; Macdonald, P. M.; Thompson, M. *Langmuir* **1994**, *10*, 492−499.
(26) Moon, J. H.; Shin, J. W.; Kim, S. Y.; Park, J. W. *Langmuir* **1996**, *12*, 4621−4624.
(27) Pihl, J.; Kabir, M. S.; Persson, S. H. M. *Mater. Res. Soc. Symp. Proc.* **2002**, *705*, 199−203.
(28) Freeman, R. G.; Grabar, K. C.; Allison, K. J.; Bright, R. M.; Davis, J. A.; Guthrie, A. P.; Hommer, M. B.; Jackson, M. A.; Smith, P. C.; et al. *Science (Washington, D. C.)* **1995**, *267*, 1629−1631.
(29) He, H. X.; Zhang, H.; Li, Q. G.; Zhu, T.; Li, S. F. Y.; Liu, Z. F. *Langmuir* **2000**, *16*, 3846−3851.
(30) Zheng, J.; Zhu, Z.; Chen, H.; Liu, Z. *Langmuir* **2000**, *16*, 4409−4412.
(31) Lin, S.-Y.; Tsai, Y.-T.; Chen, C.-C.; Lin, C.-M.; Chen, C.-h. *J. Phys. Chem. B* **2004**, *108*, 2134−2139.
(32) Lee, H.; Kepley, L. J.; Hong, H. G.; Mallouk, T. E. *J. Am. Chem. Soc.* **1988**, *110*, 618−620.
(33) Guang, C.; Hong, H. G.; Mallouk, T. E. *Acc. Chem. Res.* **1992**, *25*, 420−427.
(34) Major, J. S.; Blanchard, G. J. *Langmuir* **2001**, *17*, 1163−1168.
(35) Kohli, P.; Blanchard, G. J. *Langmuir* **2000**, *16*, 8518−8524.
(36) Kohli, P.; Blanchard, G. J. *Langmuir* **2000**, *16*, 695−701.
(37) Kohli, P.; Rini, M. C.; Major, J. S.; Blanchard, G. J. *J. Mater. Chem.* **2001**, *11*, 2996−3001.
(38) Turkevich, J.; Stevenson, P. C.; Hillier, J. *Discuss. Faraday Soc.* **1951**, *No. 11*, 55−75.

bottom flask and stirred for 24 h at room temperature, filtered, and then rinsed with water and ethanol. These reaction conditions provide a AuNP/silica particle ratio of $\sim 10^9$. The silica gel coated with AuNPs was returned to a round-bottom flask, and a 10 mM ethanolic solution of 6-mercapto-1-hexanol (10 mL) was added. The slurry was stirred at room temperature overnight. The product was filtered, rinsed with ethanol and ethyl acetate, and dried under vacuum in a round-bottom flask for a minimum of 2 h. The flask was purged with argon and then placed under vacuum again. To this round-bottom flask was added a solution of 3.5% (v/v) $POCl_3$/5% (v/v) collidine in anhydrous acetonitrile. The resulting slurry was kept under an argon atmosphere and stirred overnight. The silica gel slurry was filtered and rinsed with acetonitrile, then acetone, and distilled water. The silica gel was returned to a dry round-bottom flask. To this flask was added a solution of 5 mM $ZrOCl_2$ in 60:40 ethanol/water, and the slurry was stirred at room temperature overnight. The functionalized silica gel was filtered, rinsed with ethanol, and dried under vacuum for a minimum of 24 h prior to use. For measures of model analytes, the analytes were introduced as ethanolic solutions and the resulting slurry stirred at room temperature overnight prior to spectroscopic analysis.

UV−Visible Spectroscopy. UV−visible spectroscopy was performed using a Cary model 300 UV−visible spectrometer (Varian), with 1-nm resolution. Spectra over the range of 400−800 nm were acquired at a scan rate of 600 nm/min. Measurements were made using 3 mL of ethanolic solution (0.50 g of silica gel/5 mL of ethanol) for each measurement. The maximum absorbance for the PR was determined by integration of the spectrum.

Scanning Electron Microscopy. The samples were imaged using a JEOL JSM-6300F scanning electron microscope at 25-kV accelerating voltage. The sample was placed on a SEM stub and was sputter coated with 3 nm of gold prior to analysis.

RESULTS AND DISCUSSION

We consider four central issues in this work. These are the chemical selectivity of the AuNP-coated silica gel, the morphology of this system, the mechanism by which we observe the interaction of OPPs with the AuNP-coated silica gel, and the sensitivity of this material to the presence of OPPs. We consider these issues separately.

Chemical Selectivity. The chemistry used to achieve selective adsorption of the OPPs onto the AuNPs is, as noted above, ZP chemistry. This chemistry has been studied extensively by the Clearfield group[39−41] in the solid state and by the Mallouk, Thompson, and Katz groups[11,13,25,32,33,42−45] for binding at surfaces. It is difficult in many instances to determine the strength of the ZP bond because the equilibrium for bond formation lies far to the right, but indirect estimates of the strength of the ZP bond indicate that it is ∼60 kcal/mol or larger, under favorable conditions.[37] The issue is thus what other compounds can complex with Zr^{4+} and whether or not Zr^{4+}, once in place, can be displaced by other metal ions. Bakiamoh and Blanchard have found that $Zr(RPO_3)^{2+}$ can form complexes with RSO_3^- and RCO_2^-, but these complexes are not as strong as the $Zr(RPO_3)_2$ system.[46] While not quantitative, we believe that the formation constant for OPPs with the $Zr(RPO_3)^{2+}$-functionalized surface is sufficiently more favorable than for complexation with sulfonates and carboxylates that OPPs will displace these compounds in a competitive system. We also note that while there may be slight differences in binding efficiency for the different OPPs, in all cases, the binding to Zr^{4+} is sufficiently strong that we do not expect to observe preferential binding phenomena. These AuNP-coated silica particles are thus selective for a class of compounds rather than a specific OPP.

We are also concerned with the use of Zr^{4+} as opposed to other metal ions. There is a body of literature on the use of other metals in bisphosphonate structures, and the conclusion of that work is that most other metal ions, especially with a formal charge lower than that of Zr^{4+}, will not bind as strongly to phosphates or phosphonates.[40] The only other metal ion that is known to bind to phosphates or phosphonates as strongly is Hf^{4+}.[47−49]

Morphology. We show in Figure 2 an SEM image of silica gel particles prior to their reaction with the AuNP-containing solution. The silica particles are not regular in shape and are characterized experimentally as having an average diameter of 63.6 μm (Figure 2a). The treatment to which the silica particles are subjected appears to have a significant influence on their morphology. As can be seen in Figure 2a and b, the average particle size is substantially smaller following reaction of the silica particles with silane and AuNPs. This size reduction is advantageous as the resulting slurrys remain suspended longer than the nonfunctionalized silica gel particles. The SEM images reveal an apparent spatially heterogeneous distribution of AuNPs, implying that the surface AuNP coverage is not characterized by a homogeneous monolayer. Despite the limited resolution of our images, it is clear that the functionalized surface (Figure 3b) exhibits more roughness than the nonfunctionalized surface (Figure 3a). This rougher surface, combined with the macroscopic observation of the purple color of the silica gel, is indicative of the binding of AuNPs to the silica gel. (Attempts to further assess the surface roughness using AFM were unsuccessful due to the large difference in the relative sizes of the silica gel particle and the attached AuNPs.) A significant issue lies in understanding the reaction efficiency and resulting optical properties of the AuNPs that are bound to the silica particles, and we consider this issue next.

Characterization of the AuNP-Coated Silica. Because the optical properties of AuNPs are comparatively well understood, we use absorption spectroscopy as the basis for understanding

(39) Wang, Z.; Heising, J. M.; Clearfield, A. *J. Am. Chem. Soc.* **2003**, *125*, 10375−10383.
(40) Yang, H. C.; Aoki, K.; Hong, H. G.; Sackett, D. D.; Arendt, M. F.; Yau, S. L.; Bell, C. M.; Mallouk, T. E. *J. Am. Chem. Soc.* **1993**, *115*, 11855−11862.
(41) Ruvarac, A.; Milonjic, S.; Clearfield, A.; Garces, J. M. *J. Inorg. Nucl. Chem.* **1978**, *40*, 79−85.
(42) Hong, H. G.; Sackett, D. D.; Mallouk, T. E. *Chem. Mater.* **1991**, *3*, 521−527.
(43) Cao, G.; Garcia, M. E.; Alcala, M.; Burgess, L. F.; Mallouk, T. E. *J. Am. Chem. Soc.* **1992**, *114*, 7574−7575.
(44) Fang, M. M.; Kaschak, D. M.; Sutorik, A. C.; Mallouk, T. E. *J. Am. Chem. Soc.* **1997**, *119*, 12184−12191.
(45) Katz, H. E. *Chem. Mater.* **1994**, *6*, 2227−2232.
(46) Bakiamoh, S. B.; Blanchard, G. J. *Langmuir* **1999**, *15*, 6379−6385.
(47) Ansell, M. A.; Cogan, E. B.; Neff, G. A.; von Roeschlaub, R.; Page, C. J. *Supramol. Sci.* **1997**, *4*, 21−26.
(48) Obrien, J. T.; Zeppenfeld, A. C.; Richmond, G. L.; Page, C. J. *Langmuir* **1994**, *10*, 4657−4663.
(49) Zeppenfeld, A. C.; Fiddler, S. L.; Ham, W. K.; Klopfenstein, B. J.; Page, C. J. *J. Am. Chem. Soc.* **1994**, *116*, 9158−9165.

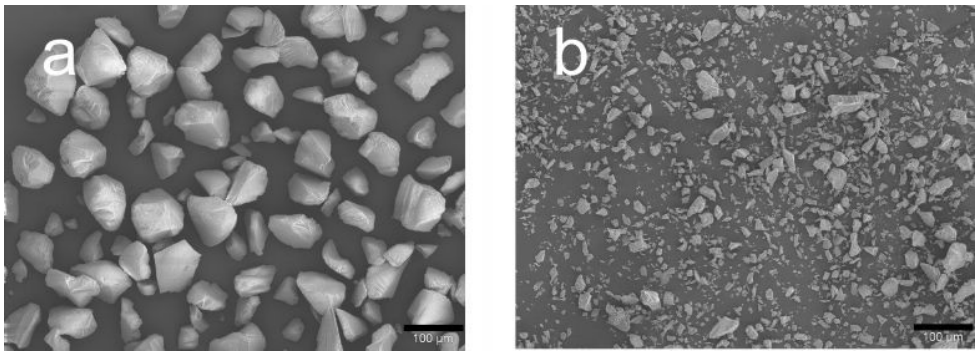

Figure 2. SEM image of (a) unfunctionalized silica gel beads with average particle size of ~63.6 μm and (b) AuNP-functionalized silica gel beads with average particle size of ~10 μm.

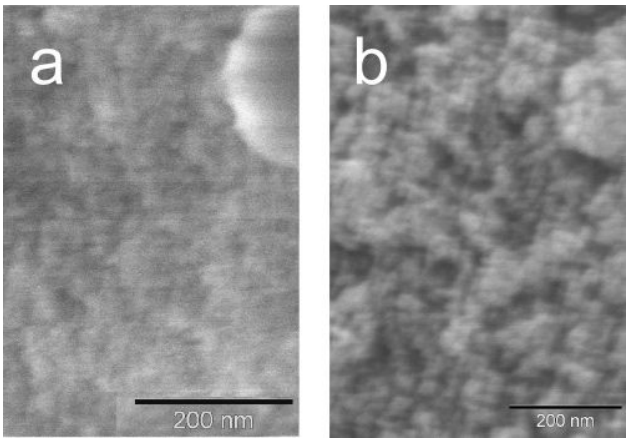

Figure 3. SEM image of the surface of (a) unfunctionalized silica gel beads and (b) AuNP-functionalized silica gel beads. The black line represents 200 nm in each image.

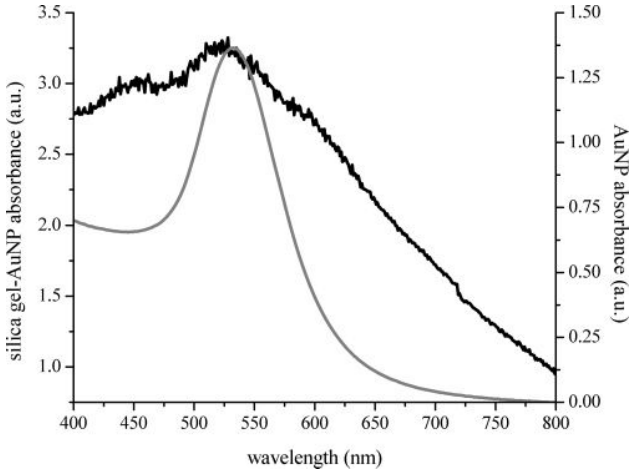

Figure 4. UV−visible spectrum of AuNP-functionalized silica gel beads with the spectrum of unfunctionalized silica gel beads subtracted in ethanol (black line) and citrate-stabilized AuNPs (gray line).

AuNP surface coverage of the silica particles. We use absorption spectroscopy to determine the amount of AuNP present and estimate the silica particle concentration and surface area based on particle size and mass used. Because of the change in silica particle size seen upon deposition of AuNPs, we provide a AuNP surface coverage range.

Using a 0.5-g sample of modified silica particles in 10 mL of ethanol, we observe the plasmon resonance band with a peak centered near 528 nm, and a background-corrected absorbance of 3.27 (Figure 4, black trace). Despite the adsorption of the AuNPs onto the silica gel substrate, there was not a significant plasmon band shift compared to the citrate-stabilized AuNPs in the same solvent (Figure 4, gray trace). The active surface of the bound AuNPs apparently experiences an environment similar to that of the unbound AuNPs. There are clearly some differences, however, as can be seen in the different band profiles for the free and bound AuNPs. The added width of the bound AuNP plasmon band could be due to a range of binding sites on the silica particles. It should also be noted here that, despite the high absorbance of 3.27, we remain well within the linear response range of our instrument, which has an upper limit of 5 absorbance units. The literature value for the extinction coefficient for 30-nm AuNPs is 4.7×10^9 L/mol·cm,[50−54] and we use this value for our nanoparticles. Using a 1-cm-path length cuvette, we recover a concentration of 6.96×10^{-10} M, which corresponds to 4.19×10^{11} AuNP/cm^3. With this AuNP loading density, we consider next the number of silica particles present and their surface area.

We note in passing that there are subtle features in the plasmon resonance spectrum for the surface-bound AuNPs at ~450 and ~580 nm (Figure 4). While the limited S/N ratio of our data and the breadth of the plasmon resonance make any detailed assignment difficult, we can speculate that there are several types of coupling of the AuNP to the silica, and the 580-nm band reflects a subgroup of AuNPs bound in a different manner. We note that this band (Figure 5) does not exhibit a positional dependence on OPP concentration. Further, more detailed spectroscopic studies could perhaps shed some light on the origin of the 580-nm band.

We place an upper bound on silica particle size by using the experimental diameter of 63.6 μm, and for the sake of simplicity, we assume spherical particles. While this is clearly not a highly accurate estimate, we are concerned here with establishing a range of surface coverage rather than determining a precise value. The volume of a 63.6-μm-diameter spherical particle is 1.35×10^{-7}

(50) Koplin, E.; Niemeyer, C. M.; Simon, U. *J. Mater. Chem.* **2006**, *16*, 1338−1344.
(51) Link, S.; El-Sayed, M. A. *J. Phys. Chem. B* **1999**, *103*, 8410−8426.
(52) Link, S.; El-Sayed, M. A. *J. Phys. Chem. B* **1999**, *103*, 4212−4217.
(53) Link, S.; Wang, Z. L.; El-Sayed, M. A. *J. Phys. Chem. B* **1999**, *103*, 3529−3533.
(54) Maye, M. M.; Han, L.; Kariuki, N. N.; Ly, N. K.; Chan, W.-B.; Luo, J.; Zhong, C.-J. *Anal. Chim. Acta* **2003**, *496*, 17−27.

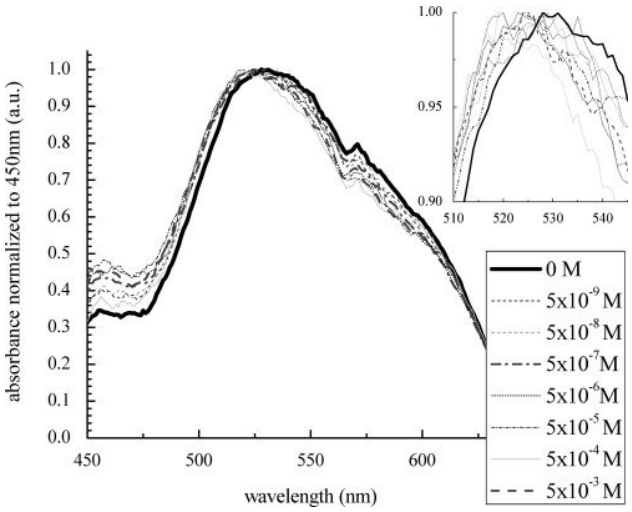

Figure 5. UV−visible spectra of silica gel sensor exposed to varying concentrations of DECP. Absorbance has been normalized to 450-nm absorbance.

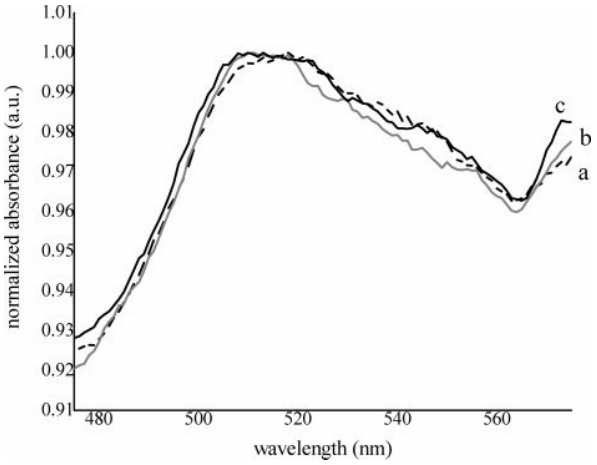

Figure 6. Response of MPTMS functionalized silica gel sensor to 24-h exposure to (a) ethanol, (b) 2 mM MPA, and (c) 2 mM DECP.

cm^3. We assume a density for the silica particle of 2.0 g/cm^3, recognizing that this is somewhat less than that of fused silica (2.2 g/cm^3). We make this estimate under the assumption that the porosity of the silica gel likely reduces its density compared to the corresponding solid material. Using a value of $\rho = 2.0$ g/cm^3, we estimate the mass of a silica particle of 2.69×10^{-7} g. In a 0.5-g sample, there are thus 1.86×10^6 particles in a 10-mL sample volume. From our estimate of 4.19×10^{11} AuNP/cm^3 and 1.86×10^5 silica particles/cm^3, we obtain 2.25×10^6 AuNP/silica particle. The size of the AuNPs we use in this work is ~10-nm radius, so the corresponding "footprint" of an AuNP is 3.14×10^{-12} cm^2/AuNP. If the silica particle were covered with a uniform monolayer of AuNPs, 4.04×10^7 AuNP would be on each silica particle. Comparing the absorbance-based estimate of 2.25×10^6 AuNP/particle to a maximum coverage of 4.04×10^7 AuNP/silica particle yields a surface coverage of 5.6% of a monolayer. If we make the same estimate as above, but using 10-μm-diameter silica particles, to more accurately reflect the reacted particle size distribution shown in Figure 2b, we estimate a silica particle density in solution of 4.77×10^7 particles/cm^3 and a surface area of 3.14×10^{-6} cm^2/particle. For these smaller silica particles, the absorbance data indicate the presence of 8784 AuNP/silica particle and a theoretical maximum coverage of 1.00×10^6 AuNP/silica particle, corresponding to a 0.8% AuNP surface coverage. From these two silica particle size limits, we see that the surface coverage ranges from 0.8 to 5.6%, depending on particle size. While it may be tempting to make a closer estimate of AuNP coverage, we believe that this would not be a useful exercise given the particle size distribution present in the samples. This range of coverages probably provides a realistic estimate of the coverage range that exists within a given sample. With this coverage range in hand, we now turn to understanding the mechanism for the AuNP plasmon band shift that is seen upon exposure to OPPs.

We observe a spectral blue-shift on complexation of the surface-modified AuNPs with OPPs. The plasmon resonance is well understood, and generally, the band position and line width are expected to vary with particle size and dielectric constant of the local environment (eq 1).[55]

$$\sigma(\omega)_{\text{abs}} = 9\frac{\omega}{c}\epsilon_{\text{m}}^{3/2}V_0\frac{\epsilon_2(\omega)}{[\epsilon_1(\omega)+\epsilon_{\text{m}}]^2+\epsilon_2(\omega)^2} \qquad (1)$$

where ϵ_{m} is the dielectric constant of the medium surrounding the nanoparticle, V_0 is the particle volume, and ϵ_1 and ϵ_2 are the real and imaginary components, respectively, of the frequency-dependent dielectric response of metallic gold.[56] For our experimental conditions, neither the particle volume nor the dielectric response of the metal is influenced to any significant extent by the binding of the OPP to the particle surface. The plasmon resonance frequency changes we observe are influenced most significantly by the dielectric constant of the AuNP immediate environment. The blue-shift we observe experimentally indicates OPP binding causes a decrease in the dielectric response of AuNP immediate environment. Based on this information, we use the blue band in the overlapped band model presented below to represent the complexed form of the ZP-coated AuNP.

Interpreting the Band Shift. We treat the measured plasmon resonance band as two spectrally overlapped bands, one associated with the free form of the AuNP and one associated with an OPP complexed to an AuNP through a ZP linkage. In this model, the spectral shift associated with complexation is due to the modulation of the dielectric response of the environment immediately surrounding the AuNP. Within the framework of this model, we assume that only one complexation event per AuNP is required to produce the observed spectral shift. If multiple complexation events were required to produce the observed band shift, the OPP concentration dependence of this effect would have a functional form different from that seen experimentally (vide infra). We consider that the complexation reaction is described by

$$\text{OPP} + \text{ZP}-\text{AuNP} \rightarrow \text{OPP}-\text{ZP}-\text{AuNP} \qquad (2)$$

$$K = [\text{OPP}-\text{ZP}-\text{AuNP}]/[\text{ZP}-\text{AuNP}][\text{OPP}] \qquad (3)$$

where OPP−ZP−AuNP is the complex between the OPP analyte

(55) Leff, D. V.; Ohara, P. C.; Heath, J. R.; Gelbart, W. M. *J. Phys. Chem.* **1995**, *99*, 7036−7041.
(56) Hoevel, H.; Fritz, S.; Hilger, A.; Kreibig, U.; Vollmer, M. *Phys. Rev. B: Condens. Matter Mater. Phys.* **1993**, *48*, 18178−18188.

Table 1. Response of Sensor to OPP Compounds Compared to the Ethanol Control Sample

analyte	PR (nm)	blue shift (nm)
2 mM MPA	516 ± 6	3
2 mM DECP	514 ± 4	4
EtOH	519 ± 2	

Table 2. Sensitivity of Sensor to DECP

DECP concn (M)	PR (nm)	blue shift from 0 mM (nm)
0	528	
5×10^{-9}	531	
5×10^{-8}	529	
5×10^{-7}	525	3
5×10^{-6}	520	8
5×10^{-5}	523	5
5×10^{-4}	518	10
1×10^{-3}	526	2
5×10^{-3}	524	4

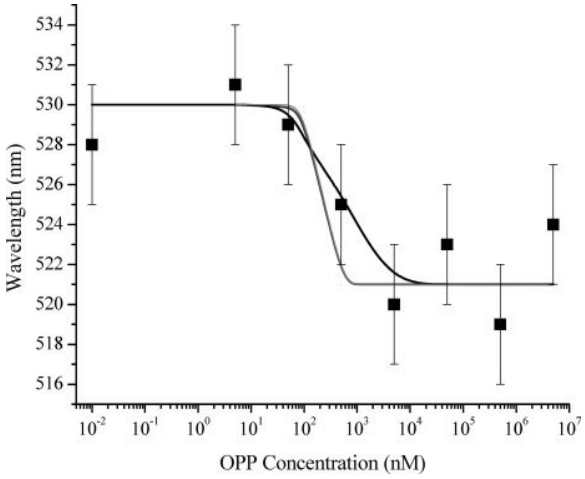

Figure 7. Comparison of observed PR bands to 1:1 free-complexed AuNP model (black trace), 2:1 free-complexed AuNP model (dark gray trace), and 3:1 model (light gray trace).

and the ZP-functionalized AuNP. The extinction coefficients of the free and complexed AuNPs are taken to be the same owing to the slight perturbation that the complexation event causes to the AuNP electronic transitions. Under this condition, the ratio of the free and complexed absorption bands is proportional to [ZP−AuNP]/[OPP−ZP−AuNP]. In this model, when [ZP−AuNP]/[OPP−ZP−AuNP] ≤ 0.1 or ≥10, the AuNP plasmon band will appear to be either that of the fully complexed form (blue band) or the free form (red band), respectively. For spectrally overlapped bands, the apparent center wavelength will correspond to the weighted average of the band maximums for the free and complexed forms. When [ZP−AuNP]/[OPP−ZP−AuNP] = 1, giving rise to a plasmon band intermediate between the free and complexed forms, $K = [\mathrm{OPP}]^{-1}$, and we observe this point experimentally for [DECP] = 5×10^{-7} M. With the value of K in hand, we can calculate [ZP−AuNP]/[OPP−ZP−AuNP] as a function of [OPP] and thus estimate the experimental plasmon band center wavelength.

Sensor Response to OPP Compounds. To determine the response of the silica gel to OPPs, we prepared 2 mM solutions of MPA and DECP in ethanol. Ten milliliters of either MPA or DECP solution was added to a clean 20=mL scintillation vial containing ~0.5 g of functionalized silica gel and a stir bar. Ten milliliters of ethanol with no analyte was added to separate vials containing 0.5 g of functionalized silica gel as a blank. For all of these measurements, the portions of functionalized silica gel used came from the same batch. The resulting slurries were stirred overnight prior to analysis to ensure completion of the ZP complexation reaction. In practice, the kinetics of ZP complex formation are fast, with Mallouk previously reporting indistinguishable results from incubation times of 1 and 24 h.[32] The sample containing no analyte demonstrated a plasmon resonance maximum at 519 ± 3 nm (1σ) (Figure 6, trace a and Table 1). Both samples containing OPPs exhibited a plasmon resonance blue-shift relative to the reference samples. The silica gel slurry with MPA analyte exhibited a plasmon resonance at 514 ± 4 nm (Figure 6, trace b and Table 1), and the silica gel slurry with DECP analyte exhibited a plasmon resonance at 516 ± 7 nm (Figure 6, trace c and Table 1), corresponding to blue-shifts of 5 and 3 nm, respectively. The uncertainties, as determined through multiple measurements of the same sample, appear relatively large, owing to the width of the plasmon resonance bands and the limited S/N available with these data due to background scattering.

The sensitivity of our coated silica particles to OPPs was evaluated using DECP as a model OPP for concentrations ranging from 5×10^{-9} to 5×10^{-3} M (Figure 5). The plasmon resonance band maximum of the analyte-exposed silica gel was compared to that of nonexposed silica gel to determine the presence and magnitude of the plasmon resonance band shift. At DECP concentrations lower than 5×10^{-7} M, the plasmon resonance band does not manifest a spectral shift outside the spectral resolution of the measurement (±1 nm) (Table 2). For DECP concentrations higher than 5×10^{-7} M (86.3 μg/L), the modified AuNP plasmon resonance exhibits a blue-shift relative to the unexposed AuNP-modified silica particles. It should be noted that the blue-shift does not appear to reach a plateau for high OPP concentration extremes. The reason for this finding lies in the uncertainty of the measurement, which depends on the substantial background scattering from the silica particles in ethanol solution. We view the sensor response as a digital response, with there being either a shift or not, making it most useful as a presumptive test for the presence or absence of OPP compounds.

We show the comparison of the experimental data to the model in Figure 7, where the solid lines are the model calculations for 1:1 OPP/AuNP (black trace), 2:1 OPP/AuNP (dark gray trace), and 3:1 OPP/AuNP (light gray trace), and the individual data points are the experimental band positions as a function of [OPP]. While there may be some contribution of 2:1 and 3:1 complexation, we believe that the correspondence between the 1:1 OPP/AuNP model and the experimental data follows the functional form of the data more closely, especially in terms of the concentration dependence. This correspondence between model and experimental data suggests that the assumption of a 1:1 OPP/AuNP complexation stoichiometry is valid. We note that there is little distinction between 2:1 and 3:1 complexation, a finding that supports the assertion that the most noticeable change in the AuNP optical response occurs for the first complexation event.

Table 3. Influence of Solvent Refractive Index on S/N Ratio and Background Absorbance

solvent	solvent refractive index	S/N	background abs (au)
EtOH	1.3614	5.8	2.5
DMF	1.4305	23.1	1.75
$CHCl_3$	1.4458	36.2	1.75
DMSO	1.4783	42.0	0.37

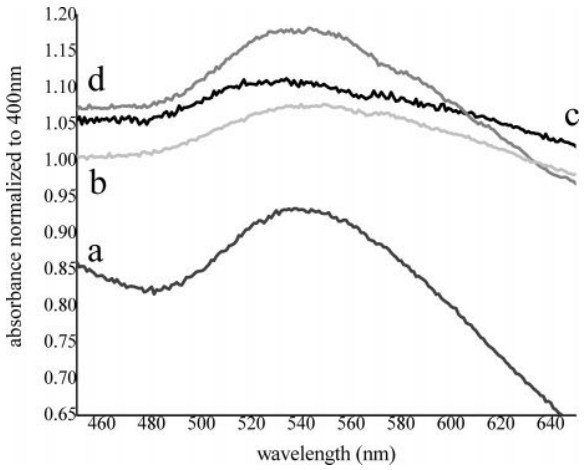

Figure 8. S/N of sensor in (a) DMSO (S/N = 42), (b) DMF (S/N = 23.1), (c) ethanol (S/N= 5.8), and (d) chloroform (S/N = 36.2).

While further complexation may occur between the AuNPs and the OPP, it appears that it will not have a significant effect on our data. We also believe that this approach to studying complexation processes holds significant promise for a number of other systems that are adaptable to surface-modification chemistry on AuNPs.

S/N Enhancement. The observed signal-to-noise ratio (S/N) for the plasmon resonance spectra of the silica gel−AuNP suspensions in ethanol prior to their exposure to an OPP was 5.8, and significantly, there was a background signal of ∼2.5 absorbance units. The attenuation of the transmitted light due to scattering loss gives rise to the large background. One way to reduce the scattering background is to use a solvent system that is better matched to the refractive index of the silica particles. The refractive index of silica gel is ∼1.46.[57] By approaching the refractive index of the immersion solvent to that of the silica gel, the S/N was enhanced because of a decrease in the observed background absorbance (Table 3). We found that, by using DMSO as the solvent (n = 1.48), we could produce a 7-fold increase in S/N compared to ethanol (n = 1.36). This increase in S/N is associated with the decreased background scattering observed from the DMSO solution to a level of 0.37 absorbance units (Table 3, Figure 8). We expect that this sort of increase in S/N and reduction in background signal will be especially beneficial in studies that focus on small concentrations of OPPs.

(57) *CRC Handbook of Chemistry and Physics,* 77 ed.; Lide, D. R., Ed.; CRC Press: Boca Raton, FL, 1996; pp 10−263.

CONCLUSION

The detection of OPPs has become increasingly important due to concerns about organophosphate/phosphonate-based chemical warfare agents and pesticides. While sensitive and class-selective detection is vital, the construction of such detection systems using simple and robust detection methodology is also of importance. The materials we have presented here, hybrid silica gel−AuNP−ZP particles, are robust and their plasmon optical response is capable of detecting comparatively low levels of OPPs complexed to the ZP termini of the particles. These materials are synthesized simply and can be made on a large scale, if required. The AuNP plasmon resonance shift we observe is independent of OPP concentration beyond a threshold concentration of $\sim 5 \times 10^{-7}$ M for DECP, corresponding to a $K \sim 2 \times 10^6$ M^{-1}. From the functional form of the plasmon resonance maximum concentration dependence, we estimate that the stoichiometry on the AuNP−ZP−OPP complex is 1:1, consistent with the estimated silica gel surface loading of 1.00×10^6 -4.04×10^7 AuNPs/silica gel particle. The sensitivity of this methodology may be improved by using a solvent system where its refractive index matches more closely the refractive index of the silica. The S/N ratio of the AuNP plasmon resonance band is improved 7-fold from 5.8 in ethanol to 42 in DMSO.

This composite material is simple to synthesize construct and utilize, and its use in the detection and sequestration of OPPs makes it useful for a host of applications in chemical warfare and pesticide analysis and remediation. The simple optical detection method we use is amenable to the incorporation of these materials in field-portable instruments. Continued improvements in the sensitivity and chemical selectivity of this novel material will afford its use as a sensor for presumptive testing for OPPs.

ACKNOWLEDGMENT

We are indebted to Dr. Ewa Danielewicz at the Michigan State University Center for Advanced Microscopy for her assistance with SEM imaging. We are grateful to the U.S. Department of Energy for their support of this work through Grant DEFG0299ER15001.

Received for review November 16, 2006. Accepted February 17, 2007.

AC062165H